

Wide Angle Light Scattering in Shock-Laser Interaction

J. Panda*

University of Toledo, Toledo, Ohio 43606

Introduction

ANY change of gas density in a flowfield is accompanied by a change in the refractive index. The sharpest change is found in a shock wave, which has a very small thickness. Light disturbances propagating across this sharp change deviate from their original path and make the shock easily visible in schlieren and shadowgraph images.¹ The net change in the index across even a strong shock is very small and, therefore, the angular deflection of the light rays is also small.² In this Note an optical phenomenon is presented where a very wide angle scattering of light is observed due to interaction between a shock wave and a laser beam. The phenomenon is described in brief in Fig. 1 where a conical shock surface and a narrow laser beam are considered. The laser beam is moved to three different axial locations parallel to the axis of the cone. It is observed that the scattered light appears in the form of a sheet at location B, where the beam is tangent (i.e., at a grazing incidence) to the shock surface. When the beam is moved to the location C, where it pierces the shock surface, the scattered light disappears. The photographic evidence, a detailed description, and the possible physical reasons behind this optical phenomenon are discussed in the text.

Experimental Setup

The present experiments were conducted in a free air jet facility³ at the NASA Lewis Research Center. High-pressure air was exhausted through a 25.4-mm-diam (D) convergent nozzle to produce various underexpanded supersonic freejets. The pressure ratio P_R (plenum pressure/atmospheric pressure) was varied between 2.42 and 5.75 to obtain various degree of underexpansion. The shock structures formed in such jets were visualized by a standard schlieren system.

The green line ($0.514\text{-}\mu\text{m}$ wavelength) of an argon-ion laser, transmitted by a fiber-optic system was used for studying the scattering phenomenon. The diameter of the beam out of the optical fiber is about 2 mm which is then focused at the jet centerline to a diameter of 0.16 mm.

Figure 2 shows a schematic of the visualization setup. The scattered light pattern was visualized on a semitransparent screen, made of a piece of translucent graph paper. The screen was mounted parallel to and 280 mm away from the jet axis. It was found that the relatively weak scattered light was difficult to observe if the main laser beam was allowed to fall directly on the screen. Therefore, a 4.8-mm-diam hole was made in the screen to allow the main beam to go through. The light pattern on the semitransparent screen was photographed by a 35-mm Nikon F4 camera, with a slow shutter speed of $1/15\text{--}1/8$ s. The complete optical setup was mounted on a 3-axis Klinger traversing unit which allowed it to be moved along the streamwise and the transverse directions.

Results

The shocks formed in an underexpanded jet of pressure ratio $P_R = 3.18$ are shown in the schlieren image of Fig. 3a. The two-dimensional projection of the shock surfaces visible in this photograph is triangular, indicating conical surfaces in the actual axisymmetric flowfield. Only the first shock surface is used to demonstrate the optical phenomenon. The locations of the laser beam with respect to this shock, for the photographs of Fig. 3b, are also indicated. The beam is normal to the plane of the paper, and the laser power used is about 70 mW.

In photograph I, the laser beam is positioned upstream of the shock and any light scattering phenomenon is absent. In photographs II and III the beam is grazing the shock surface at $z/D = -0.45$ and 0.3, respectively, where z is the radial coordinate. The normal cross sections of the scattered light appear as bright streaks spreading out from the main laser beam in both the upstream and downstream directions. The streaks are oriented along the normals to the shock surfaces which are also the direction of local refractive index gradient. Noticeably, the streaks are brighter in the downstream side of the shock. This indicates a stronger scattering in the higher density and higher refractive index side of a shock. The maximum visible value of the scattering angle θ defined as

$$\theta = \tan^{-1} \left(\frac{\text{distance on screen from center of the hole}}{\text{shock to screen distance}} \right)$$

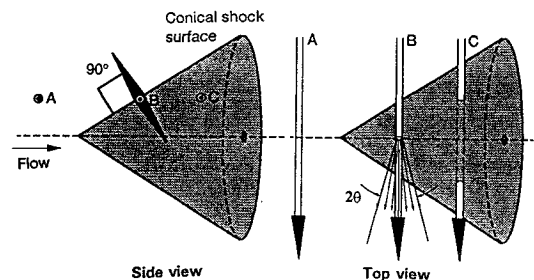


Fig. 1 Schematic of the optical phenomenon: A, B, and C are different positions of the laser beam normal to the plane of the paper in the side view and parallel in the top view.

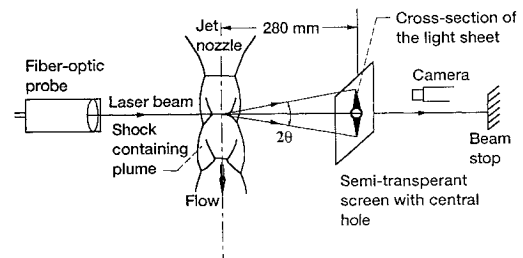


Fig. 2 Schematic of the arrangement to photograph the scattered light pattern.

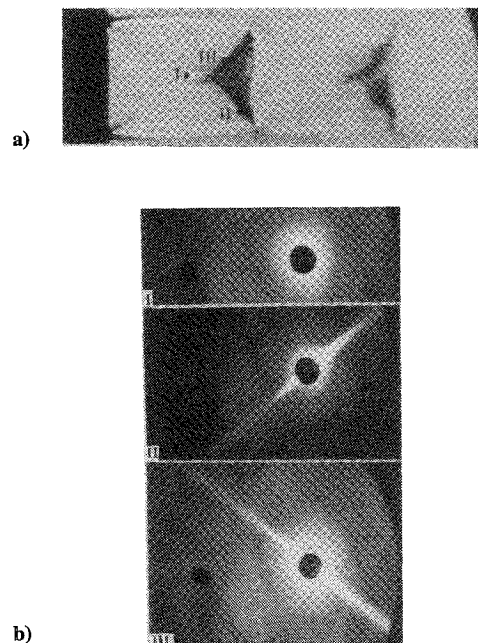


Fig. 3 a) Schlieren photograph of pressure ratio $P_R = 3.18$ underexpanded jet and locations of the laser beam and b) scattered light pattern on the screen from indicated locations.

Received June 9, 1994; revision received Feb. 14, 1995; accepted for publication Feb. 16, 1995. Copyright © 1995 by the American Institute of Aeronautics and Astronautics, Inc. All rights reserved.

*Resident Research Associate, Internal Fluid Mechanics Division, NASA Lewis Research Center, Cleveland, OH 44135. Member AIAA.

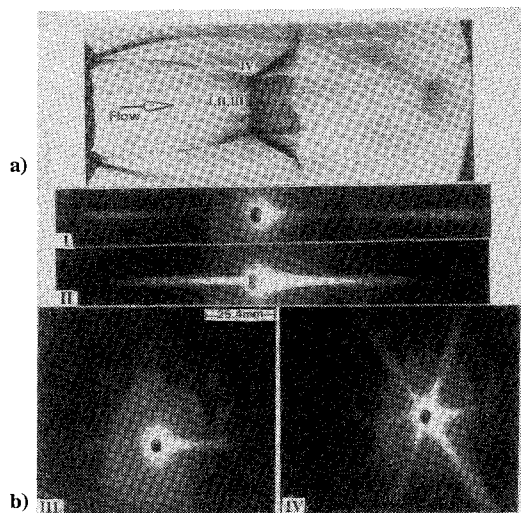


Fig. 4 a) Schlieren photograph of $P_R = 5.75$ jet and locations of the laser beam and b) scattered light pattern on the screen from indicated locations.

and calculated from photograph II is about ± 5 deg. Both the intensity and the divergence angle of the scattered light are found to increase as the shock strength is increased. It should be noted that the scattered light appears only when the laser beam is placed along the triangular trace of the shock surface shown in Fig. 3a. Along this trace, the laser beam is at a grazing incidence to the shock surface. At any other locations, where there is no shock or the beam pierces through the conical shock, the photograph of the screen is similar to that of photograph I (Fig. 3b).

Figure 4 shows photographs similar to those of Fig. 3 but for a pressure ratio of 5.75. The appearance of the shock surface is very different; a Mach disk has formed, the barrel shock from the nozzle lip to the Mach disk is clearer, and there is a reflected shock from the tip of the Mach disk to the shear layer around the jet. Photographs I, II, and III of Fig. 4b were obtained by placing the laser beam in three close positions across the Mach disk. For the latter two, the beam was moved downstream by 0.3 and 0.6 mm, respectively, from its position in photograph I. At location I the beam just touches the upstream side of the Mach disk, and the streak pattern on the screen shows definite secondary maxima on both sides. Visual investigation revealed one more maximum farther to the right beyond the width of the screen. The angular distance between the main beam and each of the secondary maxima, estimated from photograph I of Fig. 4b, is quite large, about 12.5 deg. As the beam is moved farther downstream very slowly through the shock, the secondary maxima come closer to the beam forming the continuous streak shown in photograph II. The maximum value of the visible scattering angle is still very high, about ± 10 deg. In the photograph III, the Mach disk is just left of the laser beam, and the light streak on the upstream side of the shock is very weak. In the last photograph (IV) the beam was moved to a position where all three shock surfaces (the barrel shock, the Mach disk, and the reflecting shock) merge. As expected, three intersecting streaks along directions normal to each of the shock surfaces are visible in this photograph.

The scattered light pattern is found to be independent of the polarization of the laser beam and is equally visible when a blue beam (wavelength = $0.488 \mu\text{m}$) instead of the green ($0.514 \mu\text{m}$) is used.

Discussion of Possible Physical Reasons

Since the time of first observation, various factors that may lead to light scattering were eliminated as possible reasons. The scattering phenomenon can not be caused by small particles since clean and dry air was used. Neither it can be attributed to the refractive index fluctuations caused by random turbulence, since the scattered light disappears just upstream or downstream of the shock. Another relevant concern is the effect of shock unsteadiness. The shock of Fig. 3 was oscillating by less than ± 1 mm about its mean position.³ However, the resulting oscillation of the laser beam was too small

Table 1 Estimated values of parameters relevant to the optical phenomenon observed in $P_R = 5.75$ jet, Fig. 4

Parameter	Upstream of Mach disk	Downstream
Mach no.	3.25	0.46
Static pressure, kPa	10.8	496
Density, kg/m^3	0.4	1.63
Refractive index	1.00009	1.00037
Shock thickness, μm	0.37–0.62	
Laser wavelength, μm	0.514	

to be detected, since the beam passed through the central hole on the screen independent of the appearance or disappearance of the scattered light. To determine the effect of shock unsteadiness, the light pattern on the screen was photographed by a light intensified charge coupled device camera that was gated to a fast shutter speed of 100 ns. A frame-by-frame analysis showed that the streak patterns either appear completely or disappear completely at the oscillation frequency. The instantaneous patterns also resemble those shown in Figs. 3 and 4.

To further analyze this phenomenon, various relevant parameters for the Mach disk of $P_R = 5.75$ jet (which corresponds to the photographs of Fig. 4) are estimated and shown in Table 1. The calculation procedure is described in Ref. 3. The change in the refractive index even across the Mach disk, as shown in Table 1, is small. The beam steering effect due to refraction of light across the shock is also expected to be a fraction of a degree as calculated by Kriksunov and Pliev² and measured by Faris and Byer.⁴ However, the visible spread angle of the scattered light associated with the present optical phenomenon is large, between ± 5 and ± 12 deg depending on the shock strength. Moreover, all calculations based on light refraction show that the beam bends along the direction of the refractive index gradient, whereas, for the present situation, nearly half of the scattered light appears upstream of the shock, which is opposite to such a direction.

Neither of the previous analyses consider the special situation of grazing incidence when the present optical phenomenon appears. In this condition, the shock appears as an interface parallel to the direction of propagation of the laser beam. Because of the extremely small shock thickness, the jump in refractive index is very sharp. The situation is somewhat analogous to shining a laser beam along the edge of a glass plate when a streak is observed in the far field due to diffraction of the laser by the index of refraction gradient. The streak patterns shown in the earlier figures supports this analogy. Such streaks can be considered as the Fourier transform of the step function in the refractive index caused by the shock.

Light diffraction caused by the shock waves has been observed in the shadowgraph images by Pfifer et al.⁵ (also see discussion in Merzkirch¹). A second way of looking at the diffraction phenomenon is as follows. At the grazing incidence, a part of the beam propagates upstream (lower refractive index) and the rest downstream (higher refractive index) of the shock. The difference in the optical path length between the two parts of the beam produces phase variation. Therefore, a shock wave effectively acts as a phase object⁶ that distorts the phase distribution in the laser beam. The resulting diffraction pattern is believed to manifest itself as the long streaks seen in Figs. 3 and 4.

References

- Merzkirch, W., *Flow Visualization*, Academic, New York, 1987, pp. 123–133.
- Kriksunov, L. Z., and Pliev, A. E., "Refraction of Laser Beams at a Compression Shock," *Soviet Journal of Optical Technology*, Vol. 51, No. 7, 1984; English translation Optical Society of America, 1985.
- Panda, J., "Partial Spreading of a Laser Beam into a Light Sheet by Shock Waves and Its Use as a Shock Detection Technique," NASA CR-195329, May 1994.
- Faris, G. W., and Byer, R. L., "Three-Dimensional Beam-Deflection Tomography of a Supersonic Jet," *Applied Optics*, Vol. 27, No. 24, 1988, pp. 5202–5212.

⁵Pfeifer, H. J., Vom Stein, H. D., and Koch, B., "Mathematical and Experimental Analysis of Light Diffraction on Plane Shock Waves," *Proceedings of the 9th International Congress of High-Speed Photography*, 1970, pp. 423-426.

⁶Born, M., and Wolf, E., *Principles of Optics*, 6th ed., Pergamon, Oxford, England, UK, 1989, p. 425.

Shock Detection Technique Based on Light Scattering by Shock

J. Panda*

University of Toledo, Toledo, Ohio 43606

Introduction

It has been reported in an accompanying Technical Note¹ that when a narrow laser beam is brought to a grazing incidence on a shock, a small part of the beam scatters out in a thin, diverging sheet of light. The phenomenon disappears when the beam is moved to any other location where there is no shock or the beam pierces the shock surface, i.e., at a nongrazing incidence. Various experimental details indicate that the scattering is primarily due to diffraction of light by the sudden jump in the refractive index created across a shock.

The preceding optical phenomenon is conveniently used as the basis of a new shock detection technique. It depends on moving a laser beam from point to point in a shock-containing flowfield and sensing the presence of the scattered light using a photomultiplier tube (PMT). The incident beam locations, which correspond to a nonzero PMT signal, are the shock locations. It is demonstrated that the present method is able to provide both time-averaged and unsteady information in a very straightforward way.

Experimental Setup

The present experiments were conducted in the shock-containing plume of an underexpanded, supersonic, free jet, exhausted through a 25.4-mm-diam (D) convergent nozzle, at a pressure ratio (plenum pressure/atmospheric pressure) of 3.18 (see Ref. 2). The laser beam used for the detection system is the green line ($0.514\text{-}\mu\text{m}$ wavelength) of an argon-ion laser, transmitted by a fiber-optic system. Figure 1 shows a schematic of the setup. The diameter of the beam out of the optical fiber is about 2 mm, which is then focused at the jet centerline to a diameter of 0.16 mm. The setup is similar to the one used for the visualization purpose¹ except for the light collecting and sensing devices. Just in front of the 60-mm-diam collecting lens is a 13-mm-diam beam stop that blocks the main beam. However, the diameter of the beam stop is small enough to allow most of the scattered light to enter the collecting optics. The collecting lens focuses this light to a 0.2-mm-diam pinhole that then passes it to a PMT (TSI model 9162). The electrical output from the PMT is connected across a 50- Ω terminator (not shown in Fig. 1). The voltage drop across the terminator is proportional to the PMT current and, therefore, is an indicator of the intensity of the collected light. The complete optical setup was mounted on a three-axis Klinger traversing unit that allowed it to be moved along the streamwise and the transverse directions within an accuracy of 0.025 mm. Under normal circumstances light from the laser beam does not reach the PMT. However, if the optical arrangement is moved to a location where the laser beam becomes tangential to a shock surface, a part of the scattered light is collected and sensed by the PMT, which then produces a nonzero output. The voltage signal from the PMT was digitized using a dsp Technology sample-and-hold digital converter and then stored and processed by a Microvax 3300 computer.

The detection technique is validated by comparing the shock locations identified by the present optical technique, schlieren photography, and a limited velocity measurement using laser Doppler velocimetry (LDV). The details of the one-component, fiber-optic, dual-beam, forward scatter, LDV system were reported earlier by Panda.²

Results

Figure 2 shows a comparison between the shock positions identified using this technique and those seen in a spark-schlieren photograph of the jet. The rms value of the voltage drop across the PMT, measured as the flowfield is surveyed at three radial (z) locations, are shown in Figs. 2b-2d. At $z/D = 0.45$ (close to the shear layer) the schlieren photograph indicates the presence of the shock at an axial location, $x/D = 1.2$ (the markers at the bottom of the schlieren photograph are one jet diameter apart). The laser survey (Fig. 2b) also indicates a large rms voltage around the same axial position. At the other two radial locations, centerline and $z/D = 0.2$, the scattered light is expected to appear twice, since the laser beam becomes tangential to the shock at two locations. First, when it touches the conical shock boundary and second when it touches the base of the cone. At the latter location the shock splits into many "legs" as it ends in the shear layer and any one of these "legs" can be tangential to the laser beam. The laser surveys of Figs. 2c and 2d show large rms voltages exactly around these expected locations as identified from

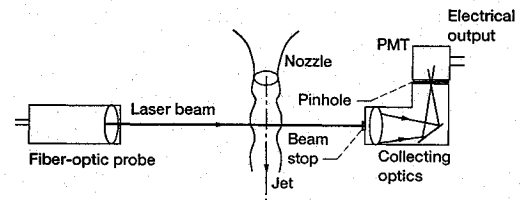


Fig. 1 Schematic of the shock detection technique.

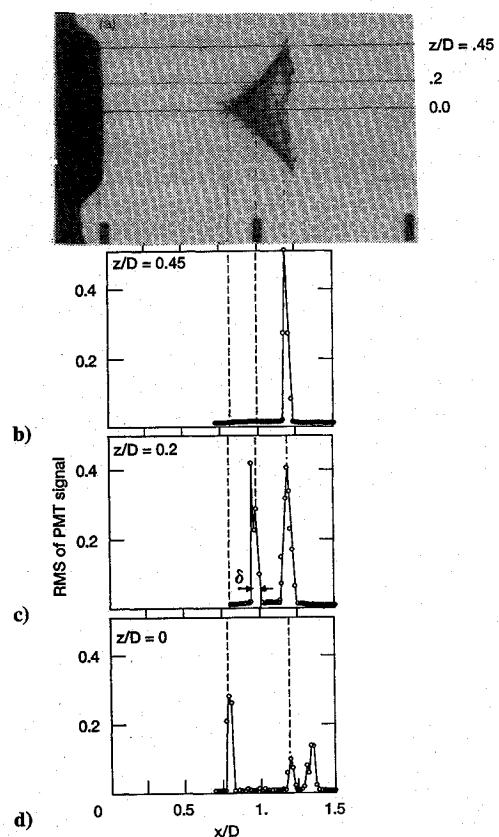


Fig. 2 Validation of the detection technique: a) schlieren photograph of shock formed in underexpanded jet; b), c), and d) laser surveys from indicated radial positions.

Received June 9, 1994; revision received Feb. 14, 1995; accepted for publication Feb. 16, 1995. Copyright © 1995 by the American Institute of Aeronautics and Astronautics, Inc. All rights reserved.

*Resident Research Associate, Internal Fluid Mechanics Division, NASA Lewis Research Center, Cleveland, OH 44135. Member AIAA.